scientific reports

Check for updates

OPEN

Quantifying the impact of surface roughness on contact angle dynamics under varying conditions

Mehdi Razavifar[1], Arastoo Abdi[2], Ehsan Nikooee[3], Omidreza Aghili[4] & Masoud Riazi[2,5]✉

Despite extensive research in recent years to clarify the role of fluid composition on reservoir wettability, understanding the properties of rock and its solid surface characteristics and their effects on wettability and its alteration remains limited and requires further investigation. This study utilized sandpaper with different roughness levels to examine the effect of roughness on the contact angles of n-heptane, crude oil (CO), brine, and deionized water (DW) with solid surfaces. In a DW-air-solid system, the measurements indicate that increasing the surface roughness beyond a certain point decreases the surface's affinity for the fluid. A similar trend was observed with the brine, although the contact angle values for the rough surfaces in contact with the brine were slightly higher than those for the DW. Increasing the surface roughness significantly decreases the contact angle between the solid and the crude oil droplet in a CO-air-solid system. In the n-heptane-air-solid system, the droplet completely spreads on the solid, regardless of the surface roughness. This variability underscores the importance of fluid-solid interactions. The CO-brine-solid system exhibits behavior similar to that of DW, with the brine generally resulting in higher contact angle values across all examined roughness levels. The examination of the contact angles for various fluids in the liquid-air-solid and liquid-liquid-solid systems shows that the contact angle depends on the mean surface roughness, the surface roughness profile, the chemistry of the fluids, and the type of fluid trapped between the droplet and the rough surface. The findings demonstrate that the effect of roughness on surface wettability cannot be interpreted solely based on the wettability of a smooth surface or the increased area due to surface roughness. The variation in the curvature of the trapped fluid can significantly influence the wettability of rough surfaces. These findings enable optimized oil recovery and flow management by demonstrating how surface roughness enhances wettability control improving oil displacement, reducing capillary trapping, and refining reservoir models. Additionally, they support engineered solutions for shale production and fouling prevention, significantly increasing operational efficiency across petroleum systems.

Keywords Contact angle, Fluid composition, Heterogeneity, Surface roughness, Wettability

Investigating fluid flow in porous media is critical for understanding flow mechanisms and developing pore-scale control methods. Key properties of porous media such as porosity, permeability, heterogeneity, and wettability must be thoroughly analyzed, as they significantly influence fluid behavior. Wettability, in particular, governs fluid saturation and production efficiency by determining how fluids interact with pore surfaces. The study of wettability dates back to Galileo's initial observations in 1612, but it was Thomas Young's pioneering work in 1805 that established the foundational principles of contact angle measurement and wetting phenomena[1]. Wettability is a critical factor in numerous industrial and natural processes, such as food processing, painting, lubrication, coating, and inkjet printing[2]. Controlling wettability is critical not only for enhanced oil recovery but also in applications involving surface adhesion and frictional interactions between grains or solids[3–5].

Wettability is determined by three key factors: surface characteristics, adjacent fluids, and their interfacial interactions. Among surface properties, roughness has been demonstrated to be the most significant. Various experimental methods exist for wettability characterization, with contact angle measurement standing out as

[1]Faculty of Chemical and Petroleum Engineering, University of Tabriz, Tabriz 5166616471, Iran. [2]Enhanced Oil Recovery (EOR) Research Centre, IOR/EOR Research Institute, Shiraz University, Shiraz, Iran. [3]Department of Civil and Environmental Engineering, School of Engineering, Shiraz University, Shiraz 7134851156, Iran. [4]Department of Petroleum Engineering, Ahvaz Faculty of Petroleum, Petroleum University of Technology (PUT), Ahvaz, Iran. [5]School of Mining and Geosciences, Nazarbayev University, Astana 010000, Kazakhstan. ✉email: masoud.riazi@nu.edu.kz

the simplest, most practical, and widely adopted quantitative approach. The fundamental understanding of roughness effects on wettability was first established through Robert Wenzel's pioneering theoretical model in 1936[6]. Wenzel's theory accounts for surface roughness effects by considering changes in both total surface area and solid-liquid interfacial area. This simple yet effective model successfully predicts contact angle variations for surfaces with simple roughness patterns and strong wetting characteristics (where $0° < \theta < 90°$). However, for contact angles in the range $90° < \theta < 180°$, the liquid fails to completely penetrate surface asperities, resulting in trapped gas pockets. This discontinuous wetting regime creates a composite interface that significantly alters both solid-liquid and gas-liquid interfacial behaviors. Cassie and Baxter (1944)[7] established a theoretical framework to describe wetting behavior on composite surfaces, explicitly accounting for air entrapment within surface asperities. While the following section provides a concise overview of these theoretical advances in roughness-mediated wettability, it is important to recognize their inherent limitations. The complex interplay between soil surface heterogeneity, fluid properties, and topographic features often exceeds the predictive capacity of such simplified models. This study addresses these limitations through systematic experimentation, specifically targeting the current models' inability to accurately represent realistic surface roughness.

Wettability quantifies a liquid's propensity to spread across a solid surface. This spreading continues until thermodynamic equilibrium is established, balancing the liquid's surface tension, gravitational forces, and capillary action. Researchers have developed numerous theoretical models and mathematical formulations to characterize surface wettability behavior[7–10]. Table 1 summarizes fundamental wettability equations, including the classical theories of Young (1805), Wenzel (1936), and Cassie-Baxter (1944). Wettability significantly influences fluid flow dynamics in porous media, governing fluid distribution patterns within rock matrices. Numerous experimental and theoretical studies have investigated how wettability alteration affects fluid transport properties. Table 2 summarizes current research findings on wettability-dependent fluid properties.

The Cassie-Baxter model explains how liquid droplets behave on rough or textured surfaces by extending Young's equation to account for roughness and air trapping beneath the droplet. It describes the apparent contact angle ($cos\theta_{\{CB\}}$) using the equation:

$$cos\theta_{\{CB\}} = f_r cos\theta_Y + f_a cos\theta_a \tag{5}$$

Where: θCB: Apparent contact angle on the rough surface (Cassie-Baxter contact angle). θY: Intrinsic contact angle on the smooth surface (Young's contact angle). fr: Fraction of the solid surface in contact with the liquid. fa: Fraction of the surface area occupied by air pockets ($fa = 1 - fr$)). θa: Contact angle of the liquid with air, which is typically 180∘ ($cos\theta_a = -1$).

The Cassie-Baxter model simplifies wettability analysis on rough surfaces by assuming: (1) a composite liquid-air-solid interface, (2) trapped air pockets minimizing liquid-solid contact, and (3) uniform roughness distribution. The model shows that wettability depends on the solid fraction (fr): when $fr = 1$, it reduces to Young's equation (complete wetting); when $fr \approx 0$, it predicts superhydrophobicity ($\theta \rightarrow 180°$). While useful for designing superhydrophobic surfaces, the model has limitations it neglects dynamic effects and assumes ideal air trapping, which may not hold for complex real surfaces. Nevertheless, it remains a foundational tool for engineering surface wettability through controlled roughness and air entrapment.

While numerous studies have investigated wettability on smooth surfaces[2,26], research addressing rough surface wettability remains limited[27]. The combined effects of surface roughness and fluid composition on wettability remain insufficiently explored in current research. Significant methodological limitations persist in experimental approaches designed to characterize roughness-dependent wettability in porous media. Many existing studies simplify their protocols by neglecting roughness effects, thereby compromising the physical relevance of their findings. Current research on surface roughness effects has predominantly examined contact angle behavior and wettability in liquid-air-solid systems, with interpretations grounded in Wenzel and Cassie-Baxter theories. However, understanding non-air trapped fluids particularly in liquid-liquid-solid systems holds critical importance for applications such as petroleum engineering, where oil-water interactions fundamentally govern enhanced recovery processes. The predominant focus on air as the trapped phase in wettability studies represents a significant limitation in understanding roughness effects. This work systematically addresses this

Theory	Equation	Application	Limitation
Young theory[7]	$\gamma_{SG} = \gamma_{SL} + \gamma_{LG} \cdot \cos\theta$ (1) γ denotes the surface tension coefficient. The subscripts SG, SL, and LG stand for solid-gas, solid-liquid, and liquid–gas interfaces, respectively The equilibrium contact angle, θ, corresponds to the minimal energy state among the three phases.	For ideally smooth and homogeneous surfaces	This theoretical relationship can't measure the contact angle of rough surfaces
Wenzel's theory[6,10]	$\cos(\theta_A) = r \cdot \cos\theta$ (2) θ_A is an apparent contact angle and θ is the angle corresponding to the ideal surface. r is the ratio of the real rough surface area to the projected ideally smooth surface	For rough surfaces	This relationship is not suitable for heterogeneous and non-uniform rough surfaces
Cassie and Baxter's theory[8,9]	$90° < \theta < 180°$ $\cos(\theta_A) = \Phi_1 \cdot \cos(\theta_1) + \Phi_2 \cdot \cos(\theta_2)$ (3) $\theta_2 = 180$ $\cos(\theta_A) = \Phi_{LS} \cdot [\cos(\theta) + 1] - 1$ (4) Φ_1 specifies the fraction of interface length and θ_1 stands for the contact angle for the first component. Φ_2 and θ_2 denote the associated values for the second component	Modeling the surface roughness effects Defines the apparent contact angle based on the fraction of interface length in the different components	This relationship is not suitable for heterogeneous and non-uniform rough surfaces

Table 1. A summary of fundamental wettability equations.

Author/year	Main target	Effective factors	Main results
Kaplan et al. 2013[8]	Investigation of the wetting behavior of stone surfaces	The salinity of water + roughness of the surface	Changing in the molecular interaction causes changes in surface roughness and increases wettability
Arsalan et al. 2015[11]	Investigation of the effects of minerals on the rock-wetting behavior	Mineralogy and rock wettability	Changing the mineral structure model and increasing the surface roughness causes an increase in wettability
Babadagli et al. 2015[12]	Investigation of the effect of surface roughness on the permeability of fractured rocks	Water and gas saturation + fluid distribution velocity + rock permeability	Changes in surface roughness and pore size increase the permeability of rock
Li et al. 2016[13]	Molecular dynamics simulations to explore the molecular mechanism for the wetting and spreading behaviors of droplets on surface roughness	Concentration of surfactant + Nanoparticles	The roughness of the bottom layer has different effects on the contact angle of nanoparticles, and the presence of surfactant reduces the droplet contact angle and changes the vapor-liquid and liquid-solid surface tensions
Scanziani et al. 2017[14]	Measurement of contact angle and fluid interface in a porous medium	The contact angle measurement in the porous media of rock	The X-ray tomography method can be used to measure the wettability of rock in the porous media
Nowrouzi et al. 2018[15]	Investigating the contact angle between the surface and fluid	Wettability of rock + fluid composition + water salinity	Increasing water salinity caused changes in surface roughness and wettability
Siddiqui et al. 2018[16]	Measurement of fluid contact angle and its effect on wettability	Physical and chemical characteristics of rock at the micro-scale + type of rock	The change in the organic compounds of the rock causes a change in the surface roughness and affects the wettability
Sun et al. 2018[17]	Investigation of the effect of water salinity on the rock wettability	Oil recovery factor + salinity of fluid + wettability	An increase in water salinity in the porous media causes an increase in wettability water absorption and oil recovery
Huang et al. 2018[18]	Investigation of the effect of the permeability model of rock and its geometric shape on the surface roughness	Fractures permeability + contact angle + roughness of rock surface	An increase in permeability causes an increase in fracture roughness and contact angle
Wang and Zhang 2020[19]	Investigation of the effect of surface roughness on the rock wettability	Performance and hydrophobic properties of minerals	Changing the molecular model changed surface roughness and strengthened the wettability of the stone
Sari et al. 2020[20]	Investigation of the role of fluid composition on the reservoir rock wettability in a multi-phase system	Fluid composition + fluid contact angle + wettability	Changes in fluid composition on the surface caused an increase in wettability and a decrease in the contact angle in multiphase systems Changing the geometric shape of the pores and the surface roughness changes the water and oil flows in the porous media of reservoir rock
Jiang et al. 2020[21]	Modeling of surface roughness of micropores and fluid flow in porous media	Surface roughness + fluid relative permeability	The tracer test can be useful in the investigation of the roughness effect on the fluid flow in the pore scale
Alnoush et al. 2021[22]	Investigating the effect of surface roughness on the wettability of calcite rock	Roughness of stone + contact angle	In calcite stones, increasing the roughness of the surface increases wettability
Nikoo and Malayeri 2021[23]	Investigation of the effect of calcium sulfate dehydrate deposition during water injection on the surface roughness	Calcium sulfate dihydrate precipitate + rock roughness + hydrophilicity of the porous media	Chemical changes in the composition of calcium sulfate dihydrate precipitate during water injection increase the contact angle and alter the wettability of the rock An increase in roughness causes an increase in polarity and causes the hydrophilicity of the porous media
Alqam et al. 2021[24]	Investigation of the effective parameters on the carbonate rock wettability	Water salinity + temperature + rock wettability + surface roughness	Injection of water with low salinity changes the surface roughness and increases rock wettability Increasing the temperature of fluid decreases the contact angle and increases the surface roughness
Sun et al. 2023[25]	Investigation of the effect of particle surface roughness on the fluid flow and surface wettability	Surface roughness + oil recovery factor + Rock wettability	Change in contact angle and surface roughness of reservoir rock changes oil recovery

Table 2. A summary of the research carried out on the wettability's effect on the fluid properties.

gap by investigating both liquid-air-solid and liquid-liquid-solid systems while characterizing heterogeneous roughness profiles. We comprehensively analyze how non-uniform surface topography influences wettability across multiple fluid systems. Our experimental approach evaluates static and dynamic contact angle behavior using four representative fluids including crude oil (CO), deionized water (DW), brine, and n-heptane on surfaces prepared with five distinct sandpaper grits (P80-P2000) to establish roughness-dependent trends. These results challenge classical wettability models (e.g., Wenzel, Cassie-Baxter), which fail to account for dynamic fluid-topography-chemistry coupling, necessitating advanced frameworks that integrate heterogeneous surface energetics, fluid polarity, and ionic dynamics. Understanding how surface roughness impacts crude oil contact angles on reservoir rocks is vital for optimizing oil recovery and flow management. Roughness modifies wettability to enhance oil displacement, reduces capillary trapping, and improves reservoir modeling accuracy. It also enables tailored engineering solutions for shale production and pipeline fouling prevention, directly boosting operational efficiency in petroleum systems.

Materials and methods

Materials

To achieve surfaces with carefully controlled and known roughness, this study utilized five different sandpapers with different roughness levels (see Table 3). These sandpapers were made of Silicon carbide. The surface roughness parameters of standard sandpaper, including RMS roughness (Sq), skewness (Ssk), kurtosis (Sku), and spatial distribution, vary with grit size and manufacturing methods. RMS roughness, which measures the root mean square of height deviations, decreases with finer grits: coarse grit (40–80) ranges from 20 to 50 µm, medium grit (100–220) from 5 to 20 µm, and fine grit (400–2000) from 1 to 5 µm. Skewness, indicating asymmetry in height distribution, shifts from slightly positive (0 to + 1) for coarse grit, due to protruding particles, to near-symmetric

Sandpaper	Mean roughness	Roughness profile
1	30.37 µm	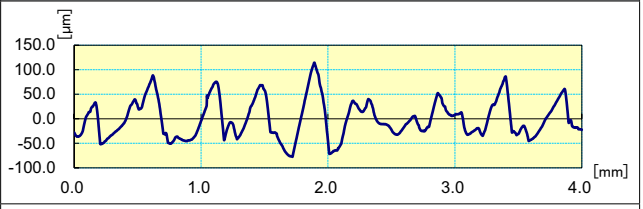
2	28.90 µm	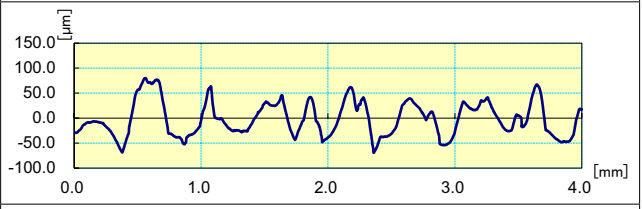
3	16.48 µm	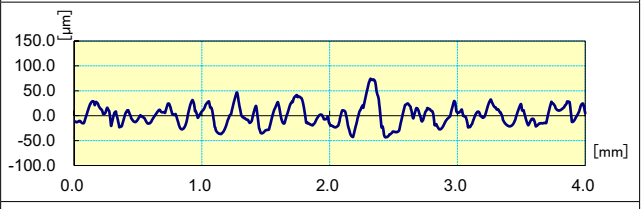
4	6.75 µm	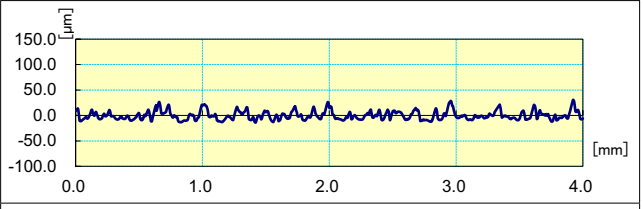
5	5.31 µm	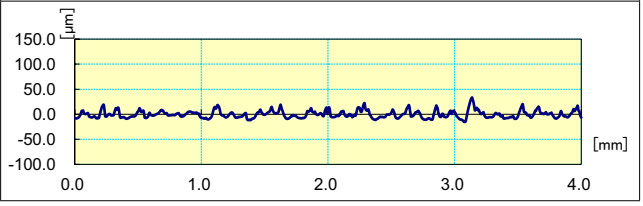

Table 3. Roughness of sandpapers used in this study.

(−0.5 to +0.5) for medium grit, and slightly negative (−1 to 0) for fine grit, reflecting smoother surfaces with fewer peaks. Kurtosis, measuring peakedness, decreases from 3 to 5 for coarse grit, with sharp peaks, to 2–4 for medium grit, and 2–3 for fine grit, which has a flatter distribution. Spatial distribution, describing particle arrangement, transitions from widely spaced, irregular patterns in coarse grit to densely packed, uniform surfaces in fine grit. Overall, as grit size decreases, surfaces become smoother, more symmetric, and less peaked, with a more uniform particle distribution.

The most common use of sandpaper is as an abrasive to remove coatings or to polish a surface with its abrasive characteristics. Sandpapers are not made of sand but rather consist of fine natural or synthetic particles. The particles (also known as grains or grit) are examined through screens and sorted by size before being bonded with an adhesive to a paper, sponge, or cloth-type backing. To achieve the desired abrasive properties, it is commonly ensured that the abrasive particles are of a specific size with little deviation.

In this study, four different liquids, whose properties are presented in Table 4, were evaluated to measure the contact angle: crude oil (CO) (from the south of Iran), deionized water (DW), brine (20000 ppm NaCl), and n-heptane (n-C7) (99% purity).

Methodology

A drop-shaped analyzer (DSA100 Krüss) was used to measure the contact angle between the different surfaces and the specified fluids. The results presented are based on the mean of two replicates, with error bars indicating the standard deviation. Contact angle measurements, conducted using DW, brine, n-heptane, and CO, were performed on surfaces with various roughness conditions. All three types of contact angles—static, advancing, and receding—were measured and reported. All measurements were taken at ambient temperature and pressure. In this regard, Fig. 1 shows a schematic of the contact angle measurement, while Fig. 2 illustrates the advancing and receding contact angles. In addition, Fig. 3 presents a schematic of the oil-water and surface contact angle measurement method.

Specification	Result				Unit
	CO	*n*-C7	DW	Brine	
Density @Ambient conditions	0.925	0.678	0.996	1.013	g/ml
Viscosity @Ambient conditions	145	0.378	0.832	–	cP
Surface tension	58.6	20.8	68.0	82.4	mN/m
Interfacial tension	CO-DW: 25.8		CO-Brine: 27.5		mN/m
Asphaltenes	8.1	–	–	–	% wt
Resins	12.9	–	–	–	% wt
Aromatics	35.6	–	–	–	% wt
Saturates	43.4	–	–	–	% wt

Table 4. Characteristics of the liquids used in this study.

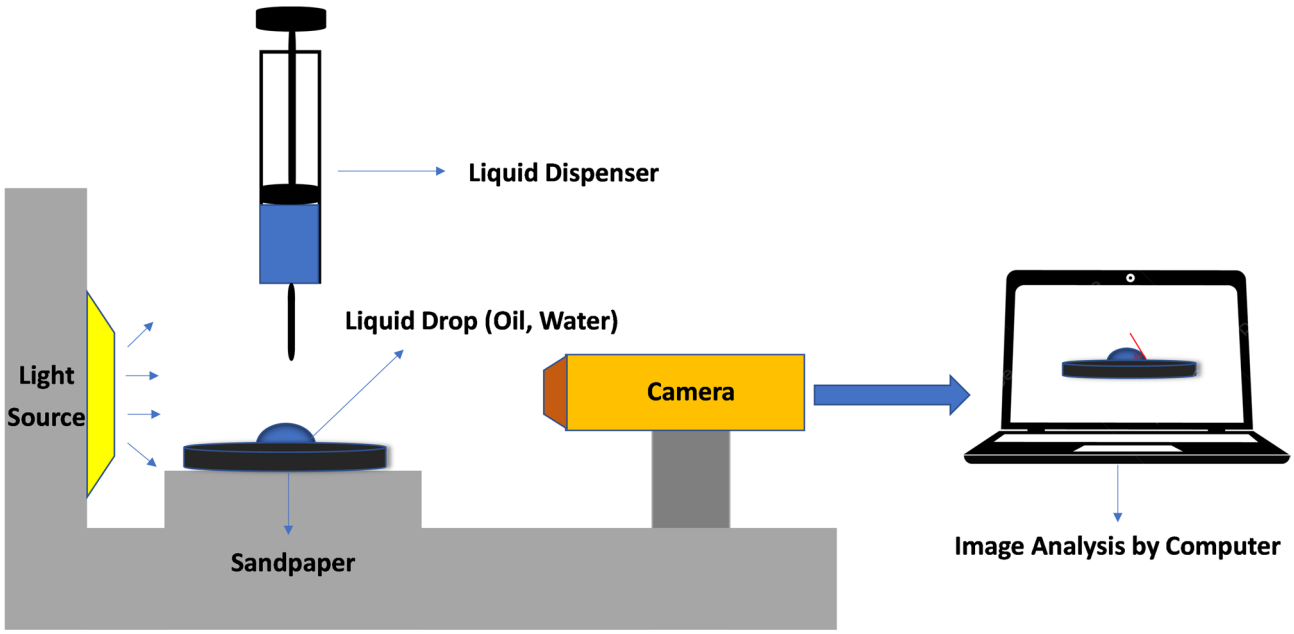

Fig. 1. A schematic illustration of the contact angle measurement method for the liquid-air-solid system.

Results

Effect of surface roughness on the contact angle measurement in the liquid-air-solid system

The effect of roughness on wettability depends on various parameters, including the fluids being evaluated. The contact angle results from the balance between the three forces that occur between two fluids and a surface. The evaluation results for different fluids including DW, brine (NaCl at 20,000 ppm), and CO are presented in Table 5 for the liquid-air-solid system, focusing on the static, receding, and advancing contact angles. In this evaluation, n-heptane was also considered; however, it is not included in Table 5 due to its complete spreading over surfaces with different roughness. The assessment of different fluids on a surface with zero roughness showed that for all four evaluated fluids (DW, brine, CO, and n-heptane), the smooth surface resulted in the complete spreading of the droplet, indicating a tendency toward perfect wettability in the liquid-air-solid system.

DW-air-solid system

The results presented for different roughness levels in the DW-air-solid system, as shown in Fig. 4, indicate that increasing the surface roughness beyond a certain point decreases the surface's affinity for the fluid. The data reveal that at high surface roughness values, the static, advancing, and receding contact angles between the solid and the water droplet are significantly higher compared to very low roughness values (Fig. 4). Although the contact angles remain below 90°, indicating a tendency of the surface toward the fluid and its hydrophilicity, the results demonstrate that the surface roughness can significantly affect the wettability. These findings contradict Wenzel's equation, which posits that if a fluid tends to wet a smooth surface (i.e., the contact angle is less than 90°), the surface's affinity for the fluid should increase with increasing roughness (resulting in a decreased contact angle)[6,28]. However, the obtained results suggest that Wenzel's equation may be uncertain when applied to surfaces with non-uniform roughness. Merely considering changes in roughness is insufficient to model variations in the resulting contact angle. Therefore, the mineralogical type of asperities becomes significant in

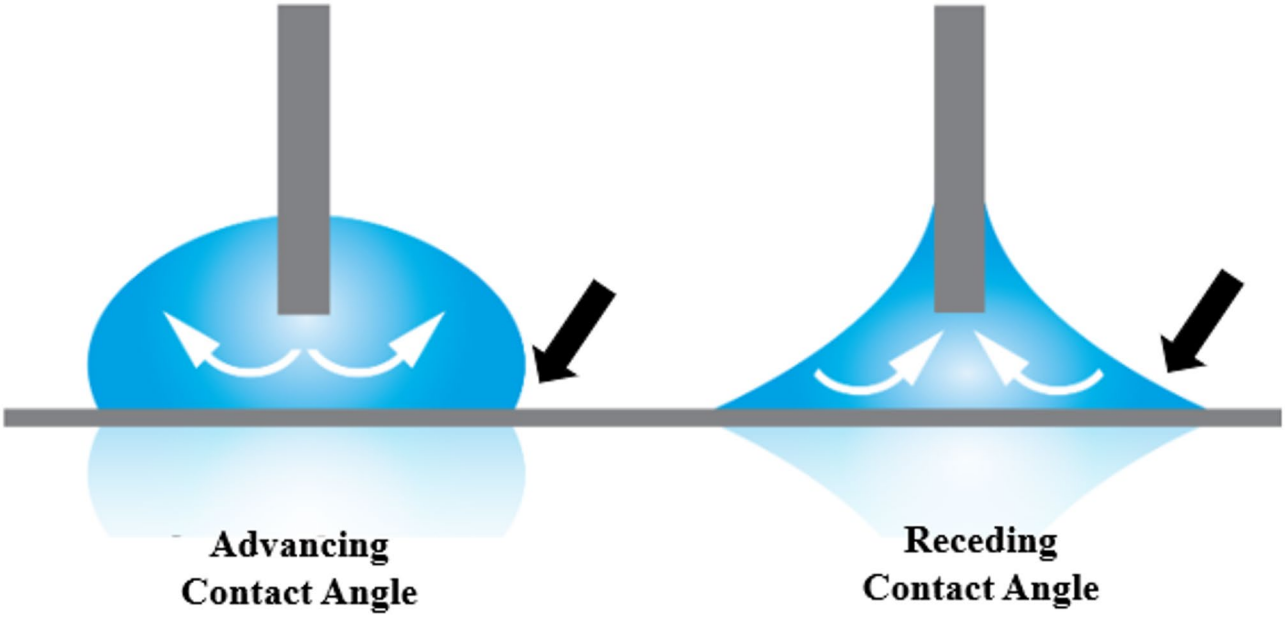

Fig. 2. Schematic of the advancing and receding contact angles.

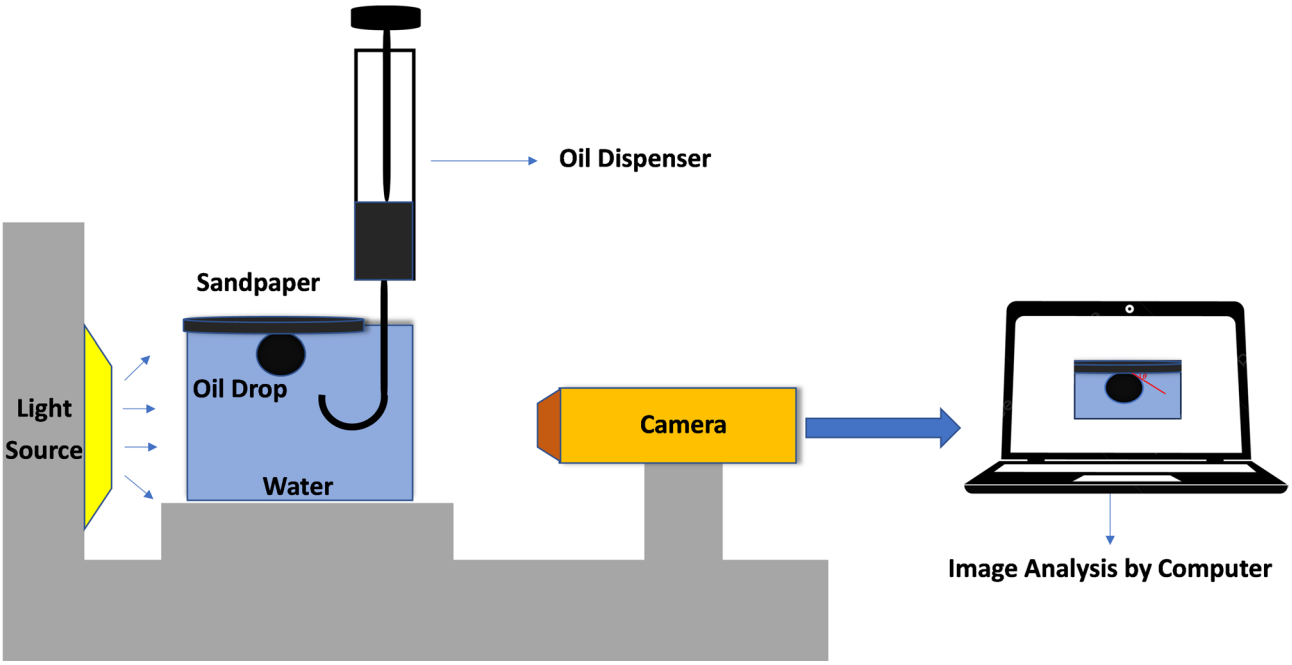

Fig. 3. Schematic illustration of the contact angle measurement method for the liquid-liquid-solid system.

natural conditions, such as rock reservoirs. Furthermore, changes in the surface roughness may arise due to the presence of heterogeneities, such as asphaltene precipitates, which indicates that alterations in the surface wettability resulting from the interplay of heterogeneity and surface roughness cannot be easily captured by simple models like those of Wenzel and Cassie-Baxter. With increasing roughness of the surface, the liquid does not fully contact the rough surface, allowing the gas molecules to become trapped in the surface asperities. These trapped gases in the rough surface prevent water from fully adsorbing on the surface.

Brine-air-solid system

The results presented in Fig. 5 show that at high surface roughness values, the static contact angle between the solid and the brine droplet is significantly higher than that observed at very low roughness values. The same trend was noted for the advancing and receding contact angles (Fig. 5). This trend is similar to that observed

Mean roughness (μm)	Static contact angle (degree)			Receding contact angle (degree)			Advancing contact angle (degree)		
	DW-Air	Brine-Air	CO-Air	DW-Air	Brine-Air	CO-Air	DW-Air	Brine-Air	CO-Air
30.37	50.79	61.40	0*	42.72	57.54	0	55.85	63.94	0
28.90	49.85	55.95	0	41.61	46.15	0	54.10	59.03	0
16.48	0	0	30.13	0	0	26.66	0	0	34.49
6.75	0	0	35.74	0	0	29.46	0	0	39.59
5.31	0	0	41.34	0	0	34.57	0	0	44.01

Table 5. Effect of surface roughness on static, receding and advancing contact angles in the liquid-air-solid system for DW, Brine, and CO under ambient conditions. *Completely spread.

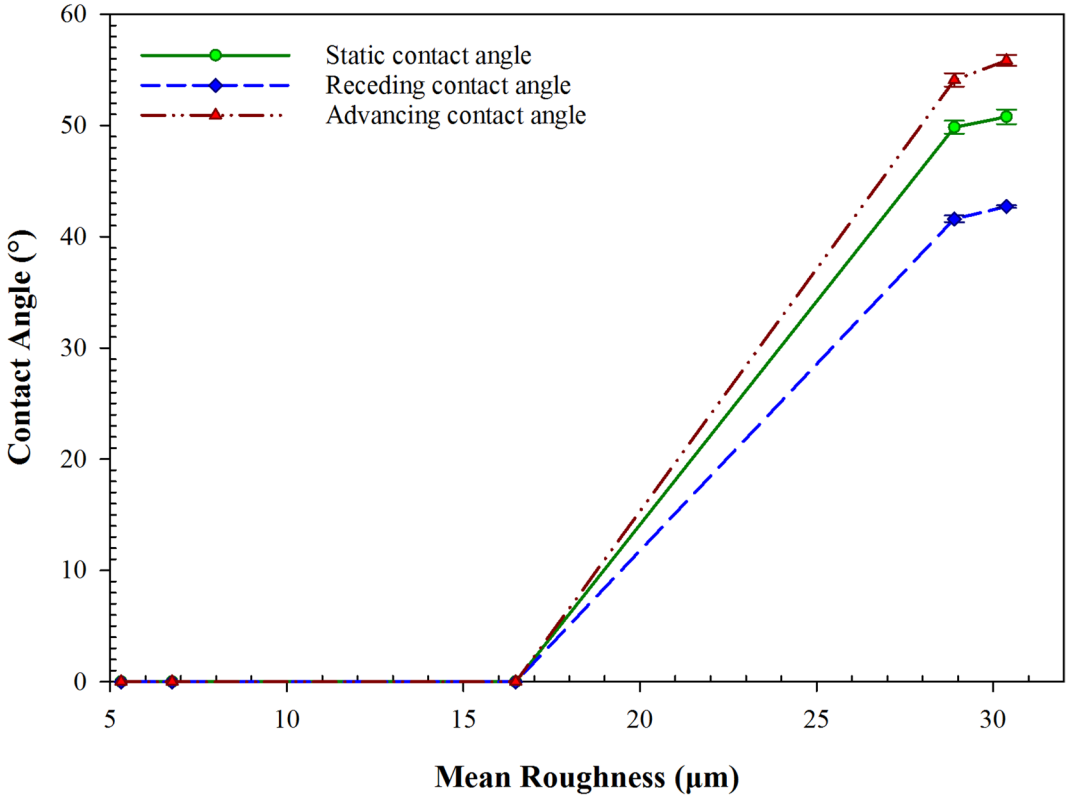

Fig. 4. Variation of the static, receding, and advancing contact angles as a function of the mean roughness for the DW-air-solid system under ambient conditions.

with DW; however, the contact angle values for rough surfaces in contact with brine are slightly higher than those for DW. These observations indicate that not only do the type of asperities and surface roughness matter, but also the fluid type, salinity, and ionic composition significantly influence the resulting wettability behavior. Changes in the surface roughness alter the interaction energy between the fluid and the solid surface, which, in turn, affects the fluid's absorption on the surface and its wettability[23].

Crude oil-air-solid system

According to the results, generally speaking, as the surface roughness increases, the static contact angle between the solid and the crude oil droplet significantly decreases (Fig. 6). The same trend was observed for the advancing and receding contact angles. A different trend with varying fluid types highlights the role of fluid-solid interactions. This trend is almost the opposite of what is observed for DW and brine, where higher contact angle values correspond to surfaces with greater mean roughness. This observation can once again be attributed to the surface properties of the asperities, indicating that oil droplet spreading is favored by increased surface roughness, which leads to a larger oil-surface contact area. Rough materials possess a greater total surface area compared to smooth ones, primarily because of their micro-depressions. This increased surface area enhances the wettability. When a droplet rests on a rough surface, the wetted area exceeds the simple geometric area due to the irregularities. Consequently, this leads to a more significant increase in the surface energy during the wetting process[29].

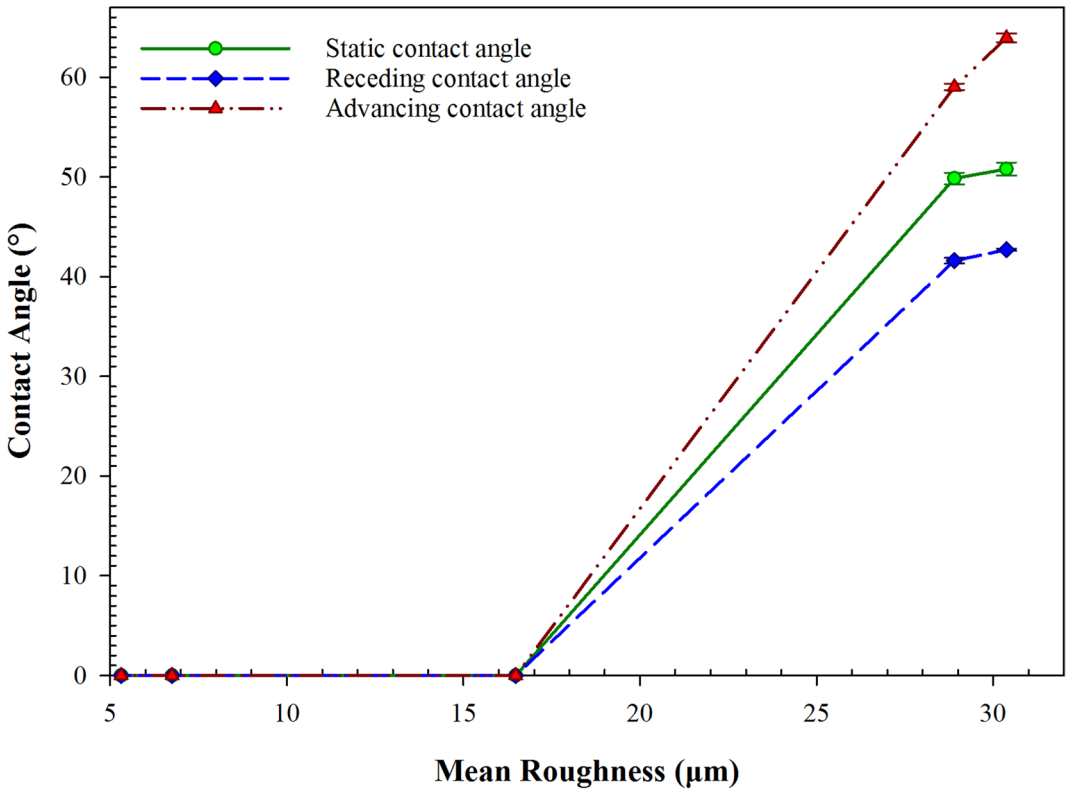

Fig. 5. Variation of the static, receding, and advancing contact angles as a function of the mean roughness for the brine-air-solid system under ambient conditions.

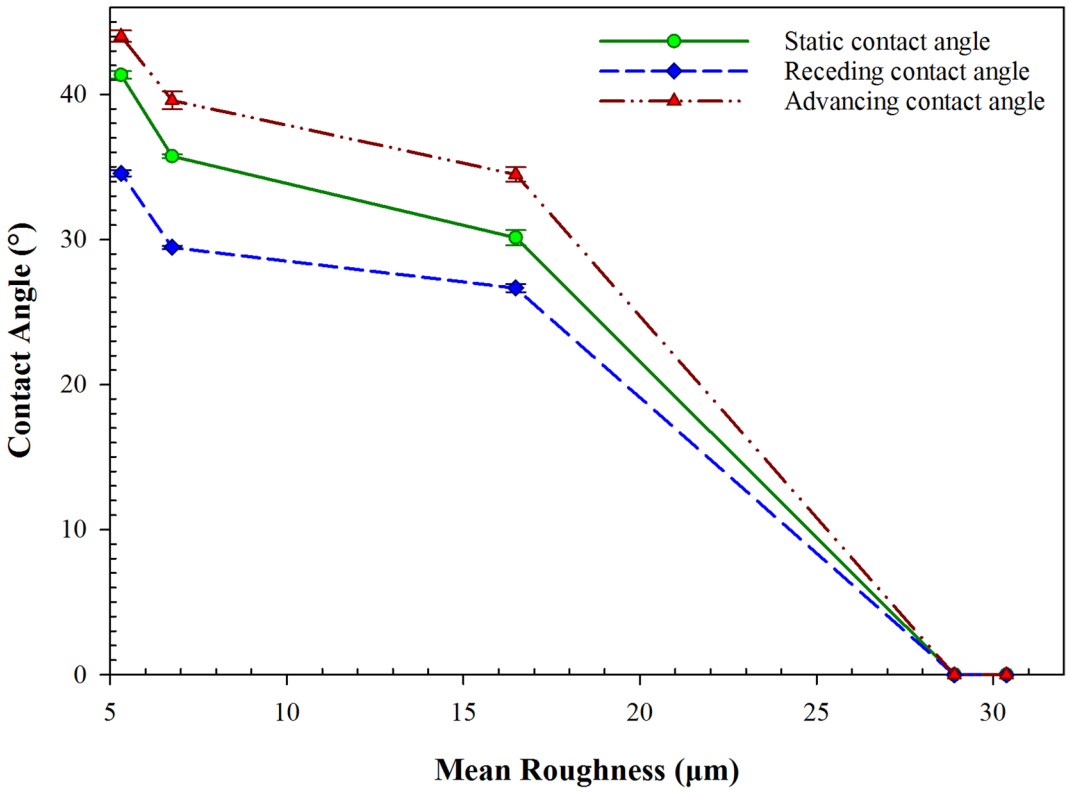

Fig. 6. Variation of the static, receding, and advancing contact angles as a function of the mean roughness for the CO-air-solid system under ambient conditions.

Mean roughness (μm)	Static contact angle (degree)	
	CO-DW	CO-Brine
30.37	44.40	34.35
28.90	34.20	30.47
16.48	30.60	27.85
6.75	26.30	23.43
5.31	23.00	19.78
0	17.70	14.23

Table 6. The effect of surface roughness on the static contact angle in the liquid-liquid-solid system for CO/DW and CO/brine under ambient conditions.

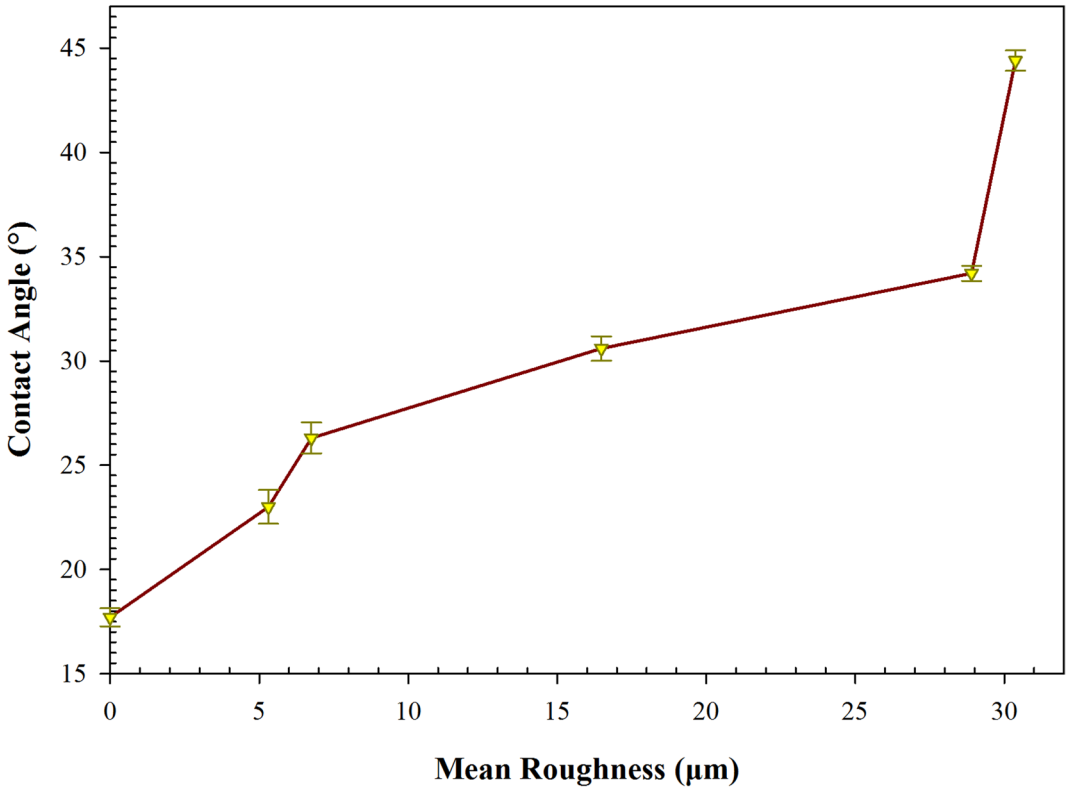

Fig. 7. Variation of the static contact angle as a function of the mean roughness for the CO-DW-solid system under ambient conditions.

N-heptane-air-solid system

In the n-heptane-air-solid system, the drop was completely spread on the solid regardless of the surface roughness.

Effect of surface roughness on the contact angle measurement in the liquid-liquid-solid system

Crude oil-DW-solid system

The evaluation of different fluids demonstrated that they can significantly affect the behavior of the contact angle in various roughness conditions for the liquid-air-solid system. In the investigated systems, air served as a non-wetting fluid, while the fluids examined DW, brine, CO, and n-heptane were considered the wetting phase in comparison to air. To investigate the effect of roughness on the contact angle in the presence of two liquids and surfaces, CO was evaluated alongside DW and brine, with the results presented in Table 6. The variety of fluids covering the bulk of the surface and surrounding the droplet can yield different results depending on the distinct forces acting compared to air.

The static contact angle results presented in Fig. 7 for the CO-DW-solid system exhibit an increasing trend with increasing roughness. These results indicate that the rough surface has a greater affinity for water, resulting in lower contact angle values. However, the increase in roughness also caused the surface to be less attracted to

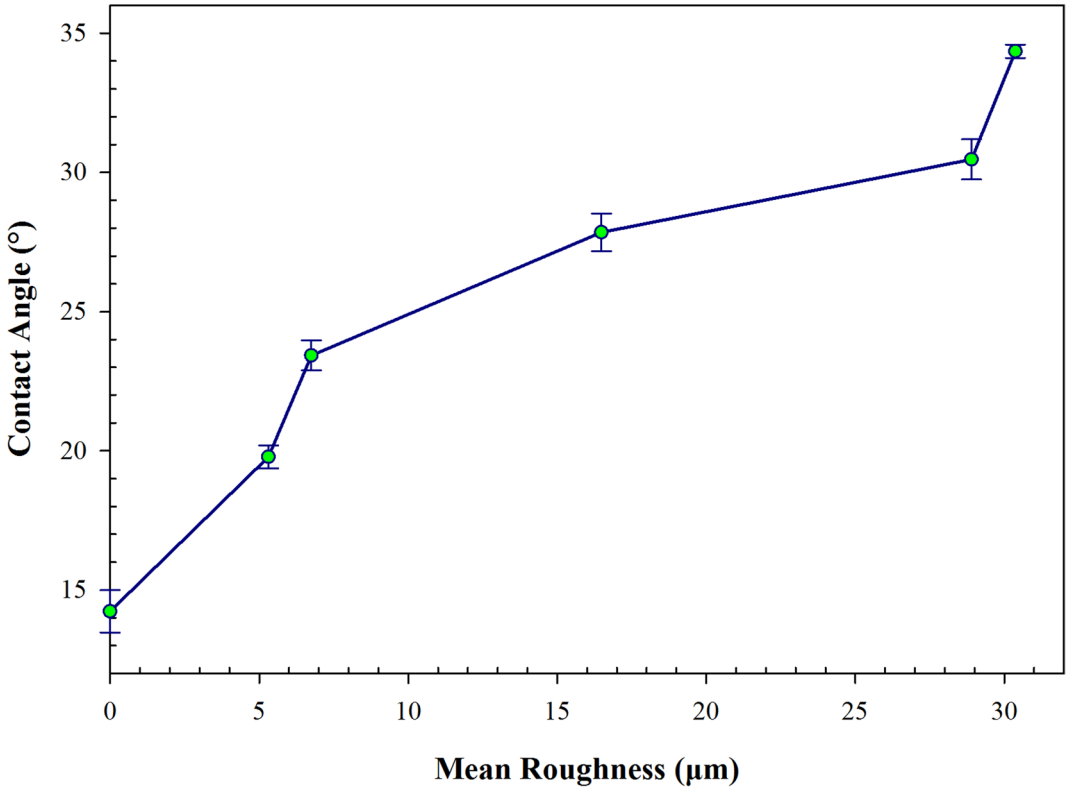

Fig. 8. Variation of the static contact angle as a function of the mean roughness for the CO-brine-solid system under ambient conditions.

Modeling parameters	Static contact angle					Receding the contact angle			Advancing the contact angle		
	DW-Air	Brine-Air	CO-Air	CO-DW	CO-Brine	DW-Air	Brine-Air	CO-Air	DW-Air	Brine-Air	CO-Air
R	1	1	0.9969	1	1	0.9988	1	0.9979	1	0.9782	0.9964
R^2	1	1	0.9937	1	1	0.9976	1	0.9957	1	0.9570	0.9928
R^2_{adj}	1	1	0.9686	NaN	NaN	NaN	NaN	0.9786	NaN	NaN	0.9639

Table 7. Match the parameters of the experimental data with the empirical model for different systems and fluids.

water in the presence of oil, leading to a change in wettability from highly water-wet to less water-wet (more oil-wet). Although the wettability across surfaces with a roughness of 30.37 μm considered significant still reflects the hydrophilicity of the surface, the increase in roughness promotes the tendency of the surface to allow oil droplets to spread more readily at higher roughness levels.

Crude oil-brine-solid system

The results presented in Fig. 8 for the CO-brine-solid system exhibit behavior similar to that of DW, with the notable difference that brine generally results in higher contact angle values across all examined roughness levels. The difference in the contact angle values between the brine and DW can be attributed to the presence of salt in the water phase, which reduces the surface's affinity for water. These results indicate that the chemistry of the studied fluid can significantly influence the contact angle outcomes, as changes in the nature of the fluid alter the forces affecting the contact angle and wettability. The findings illustrated in Fig. 8 demonstrate that the presence of salt decreases the hydrophilicity of the surface.

Empirical modeling

The experimental results indicate that static, receding, and advancing contact angles can behave differently depending on the type of fluid, surface roughness, and the investigated system. Therefore, based on the obtained experimental results, an empirical model was developed using Sigma Plot software (version 14) for both liquid-air-solid and liquid-liquid-solid systems, as described in Equation 6. The close alignment of Equation with the experimental results, evaluated using the parameters of data fit (R, R^2, and $R_{adj}{}^2$ presented in Table 7, demonstrates a strong correlation between the model and the data for both the liquid-air-solid and liquid-liquid systems.

The R, R^2, and R_{adj}^2 values indicate that the proposed model effectively describes the relationship between the independent and dependent variables. Furthermore, the type of fluid significantly influences the behavior of the contact angles (static, receding, and advancing). This influence is reflected in the constant coefficients of the experimental model, which are provided separately in Table 8 for each fluid and system examined in this study.

$$\theta_m = \frac{a + (b \times R_a) + \left(c \times R_a^2\right)}{1 + (d \times R_a) + (e \times R_a^2) + (f \times R_a^3)} \tag{6}$$

θ_m: Contact angle (static, receding, advancing) of the model for the liquid-air-solid and liquid-liquid-solid systems (°), R_a: Mean roughness (µm).

Quantitative comparison between experimental contact angles and theoretical predictions from Wenzel/Cassie-Baxter models is not appropriate or practical due to the models' idealized assumptions. These models presume homogeneous roughness, uniform fluid interactions, and static equilibrium, whereas our surfaces exhibit heterogeneous roughness (varied asperity sizes/shapes), chemical heterogeneity, and dynamic wetting behavior. Additionally, key parameters like roughness ratios (r) or fractional contact areas (f_1/f_2) are challenging to measure accurately, while multi-scale roughness and time-dependent effects (evaporation, aging) further deviate from model assumptions. Such discrepancies arise from oversimplified theoretical frameworks that ignore localized wetting states, fluid variability, and hierarchical surface structures.

Discussion

Evaluation of the Wenzel and Cassie-Baxter equations

The evaluation of the obtained results showed that the contact angle for surfaces with heterogeneous roughness across different systems and fluids can yield varying results. Investigating the details of the surface, the system in question, and the fluid being studied can be crucial in determining the observed behaviors. Literature studies have used the Wenzel and Cassie-Baxter equations to examine roughness and its effect on wettability. However, various studies, including those by Mchale[30], Liu et al.[31], Marmur and Bittoun[32], and Gao and Mccarthy[33], have indicated that determining the wettability and contact angle using these equations can lead to uncertainty. Li et al.[34] assessed the contact angle on surfaces with different roughness using molecular dynamics simulations and stated that Wenzel's equation is applicable under conditions where the surface has homogeneous roughness, uniform roughness height, and a consistent distribution of roughness across the surface. They also noted that the Cassie-Baxter equation applies in scenarios with homogeneous roughness, the same roughness height, uniform distribution, and the absence of curvature between the trapped fluid and the droplet on the rough surface[34]. In contrast, the evaluation results in the present study pertain to surfaces with heterogeneous roughness and non-uniform roughness heights, which, according to the obtained results, do not align with the conditions required for the applicability of the Wenzel and Cassie-Baxter equations. Therefore, the results obtained in this study did not meet the expectations set by these equations.

Evaluation of the effect of surface roughness on contact angle

The results presented in this study demonstrate that heterogeneous surface roughness can behave differently with various fluids across different systems. The reasons for this variability can be attributed to the surface characteristics, fluid properties, and the interactions between the surface and the fluids, as well as the interactions among the fluids themselves. Given that the chemical properties of the examined surfaces were consistent, changes in the surface roughness represented as the mean surface roughness in Table 3, along with variations in the height of the surface roughness significantly impacted the contact angle and wettability. In addition to the surface roughness parameter, the roughness profile itself can also influence the results. The non-uniform roughness of the surface complicates the environment in which the droplet contacts the surface, making the contact line between the droplet and the surface difficult to identify. This complexity varies with changes in the height of the non-uniform roughness beneath the droplet, indicating that the surface roughness profile has a significant effect on the contact angle[35,36].

The impact of the interactions between the fluids and the surfaces, as well as the interactions among the fluids themselves, is another factor affecting the contact angle, which was investigated through various fluids and systems. When the surface is part of the liquid-air-solid system, air is considered a non-wetting fluid compared to DW, brine, CO, and n-heptane. Air trapping can occur beneath the droplet and between the rough surface

	Static contact angle					Receding the contact angle			Advancing the contact angle		
Coefficient	DW-Air	Brine-Air	CO-Air	CO-DW	CO-Brine	DW-Air	Brine-Air	CO-Air	DW-Air	Brine-Air	CO-Air
a	−0.0013	−0.0018	−0.2278	17.7	14.23	−6.83E−14	−0.0021	−0.1385	0.0006	1.60E−13	−0.2216
b	9.21E−05	0.0001	−5.8367	−2.4491	−1.9629	7.11E−13	0.0002	−4.9035	−0.0002	−5.89E−14	−7.21
c	0	0	0.1986	6.94E−02	0.0677	−4.67E−14	0	0.1667	1.19E−5	2.86E−15	0.2452
d	−0.0675	−0.0675	−0.3780	−1.75E−01	−0.1811	−0.0002	−0.0675	−0.3810	−0.0002	−0.0494	−0.4007
e	0.0011	0.0011	0.0142	0.0084	0.0096	−0.0034	0.0011	0.0146	−0.0034	−8.80E−5	0.0152
f	0	0	0	−0.0001	−0.0001	−7.67E−5	0	0	−7.67E−5	2.07E−5	0

Table 8. Constant coefficients of the empirical model for various systems and fluids.

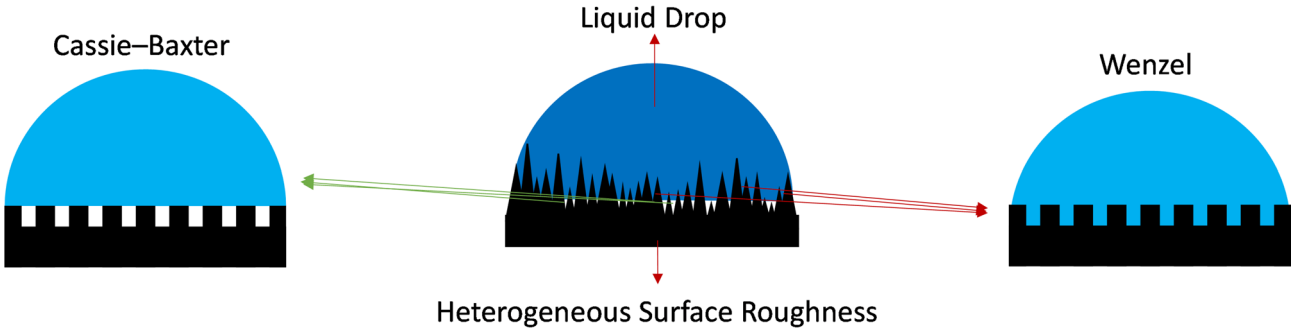

Fig. 9. Schematic representation of the droplet placement on a heterogeneous rough surface.

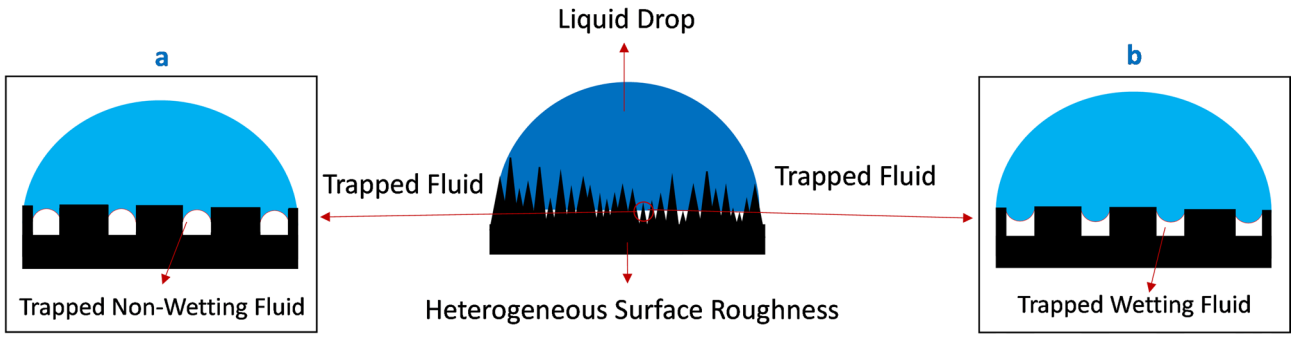

Fig. 10. Schematic representation of the curvature of the trapped fluid on the surface roughness for (**a**) non-wetting trapped fluid and (**b**) wetting trapped fluid.

and the droplet. Due to the non-uniformity of the rough surface, as illustrated in Fig. 9, some contact areas of the droplet with the rough surface may be free from air trapping, aligning with the assumptions of the Wenzel equation. However, in overlapping areas between the rough surface and the droplet, air may also be trapped, which corresponds to the assumptions of the Cassie-Baxter equation. These behaviors indicate that it is possible for the assumptions of both the Wenzel and Cassie-Baxter equations to coexist in the studied systems.

Additionally, the effects of the fluid and non-uniform surface roughness are not the only considerations. The tension between the droplet and the air, aside from the surface of the droplet which is relevant in the equation for determining the contact angle can also occur between the droplet and the trapped air, as shown in the schematic in Fig. 10. When air is trapped beneath the droplet, it functions as a non-wetting fluid. The curvature of the fluid between the trapped air and the droplet is depicted in Fig. 10a. This curvature can influence the contact angle based on the scale of the examined roughness at the point of contact between the surface and the bulk.

Examining the results of the liquid-liquid-solid system, influenced by different interactions between the liquids instead of air-liquid interactions, yielded varied outcomes. The results obtained for the CO-DW-solid and CO-brine-solid systems at zero roughness indicated that the surfaces were extremely hydrophilic, with a greater affinity for DW and brine than for CO. This tendency results in the liquid-liquid curvature across different roughness levels, as depicted in Fig. 10b. This curvature arises from the surface's affinity for DW and brine. However, in addition to the shape of the curvature created between the liquid-liquid phases and the rough surface, the roughness profile and the nature of the fluids also influence the resulting curvature. The characteristics of the trapped fluid and the droplet can affect the degree of curvature produced[37,38]. Furthermore, the surface roughness plays a role in shaping this curvature. The results indicate that when the trapped fluid is a non-wetting fluid, as shown in the schematic of Fig. 10a, the resulting curvature can contribute to a reduction in the contact angle, provided that the trapped fluid has a lower density (Fig. 10b). Conversely, when a wetting fluid is trapped, it can increase the contact angle, provided that the trapped fluid is denser. Additionally, the curvature may change with an increase in the average surface roughness and roughness height, thereby affecting the contact angle.

The materials discussed have shown results for static, advancing, and receding contact angles in liquid-air-solid and liquid-liquid-solid systems, influenced by the mean roughness, roughness profile, the fluid evaluated as a droplet on the surface, and the fluid present in the bulk of the droplet and on the surface (essentially, the system being evaluated). The curvature between the trapped fluid and the droplet will depend on the surface roughness and whether the trapped fluid is wet or non-wetting[37,38]. The curvature created in the surface roughness between the two fluids can also be influenced by the nature of the fluids, the surface roughness itself, the wettability of the fluids, and the interfacial tension between them. These parameters indicate that predicting the contact angle

for surfaces with heterogeneous roughness using the Wenzel and Cassie-Baxter equations will involve a degree of uncertainty.

The interaction between two fluids on a rough surface is governed by capillary forces. When a droplet is placed on a rough surface with various peaks and valleys, and the bulk of a fluid is immiscible with the droplet, the behavior of the droplet within the surface pores is influenced by these capillary forces. The capillary force generated can be affected by the shape of the pore and the curvature between the two fluids (the droplet and the trapped fluid). Under these conditions, the contact angle can be influenced by the properties of the surface and the fluids, as well as the interactions between the surface and the fluids themselves. Dullien has expressed the effect of pore structure including the pore radius at the wetting front (R), the convergence angle of the pores (φ), and the curvature of the interface (r_c) on the contact angle as shown in Eq. (3)[8]. This equation illustrates the interactions between the surface-fluid and fluid-fluid in the pores and on the rough surface. The contact angle of a droplet on a rough surface, when another fluid is trapped beneath it, can be affected by all three parameters outlined in Equation, which can alter the contact angle. The schematic in Fig. 11 illustrates the separate effects of each parameter: R, r_c, and φ. In this study, the contact angle of a droplet on a rough surface, according to the roughness profile shown in Table 3, causes the effects depicted in Fig. 11 to occur simultaneously, resulting in complex behavior for the contact angle. The significance of fluid curvature on the contact angle, as shown in Fig. 10, can vary depending on the trapped fluid. Behnoudfar et al.[37] demonstrated that the contact angle in a porous medium is influenced by fluid-fluid curvature and the pore radius (an indicator of surface roughness in this study), and that a non-wetting fluid can significantly impact the contact angle. The findings of Behnoudfar et al.[37], in line with the present study, confirm that fluid curvature and the type of trapped fluid which causes changes in fluid curvature (illustrated in Fig. 10) have a significant effect on the contact angle.

Performing advancing and receding contact angle tests on a rough surface involves the interaction of the droplet and bulk fluid within the pores of that surface, manifesting as imbibition or drainage processes. These processes can occur for either advancing or receding contact angles, depending on the type of trapped fluid. In the present study, since the advancing and receding contact angles are evaluated in a liquid-air-solid system, the bulk fluid (air) will always be a non-wetting phase. In the evaluation of the advancing contact angle, increasing the volume of fluid in the droplet causes the droplet fluid (DW, brine, CO) to replace air in the pores of the rough surface, representing the imbibition process. Conversely, during the assessment of the receding contact angle, the wet phase gives way to air (the non-wetting phase), representing the drainage process. These processes are significant depending on the tendency of the rough surface to trap the fluid. The receding contact angle is highly sensitive to structural parameters such as pillar height, spacing, and pore size, showing unique trends for each structure. Increasing pore size reduces the solid-liquid contact area, raising the droplet depinning force. Unlike filled pillars, pores hinder contact line sliding, enhancing interface distortion and adhesion[35]. In the present study, considering that the drainage process occurs during the assessment of the receding contact angle, capillary pressure acts as a factor opposing the movement of the droplet contact line. This capillary pressure, known as negative pressure within the pore, is generated during the evaluation of the receding contact angle. It is essentially the same negative capillary pressure encountered during the drainage process, which must be overcome by an external force. The drainage behavior observed during the assessment of the receding contact angle causes the three-phase contact line to become pinned, requiring additional force to overcome both the structural forces and the capillary pressure, as strong adhesion develops due to the pinning of the contact line. The primary mechanism behind the high adhesion is strong contact line pinning, where the droplet's edge becomes anchored to microscopic surface features, preventing its motion[36]. The high adhesion observed in this state is attributed to the unique surface geometry, which traps air pockets and pins water droplets in place[39]. This negative pressure depends on the type of trapped fluid, which can play an important role in the contact angle. However, this negative pressure does not always arise during the evaluation of the receding contact angle; it occurs only when the trapped fluid is a non-wetting fluid, as illustrated in the schematic shown in Fig. 10a. The evaluation of the advancing contact angle in the present study, which represents the imbibition process, is the opposite of the drainage process. In this case, the capillary pressure acts as an auxiliary force, facilitating the penetration of the droplet fluid into the pores of the rough surface and creating positive pressure in the direction of the three-phase contact line. Literature studies investigating roughness have primarily focused on the negative pressure created during the assessment of the receding contact angle[35–37,40]. However, according to the schematic

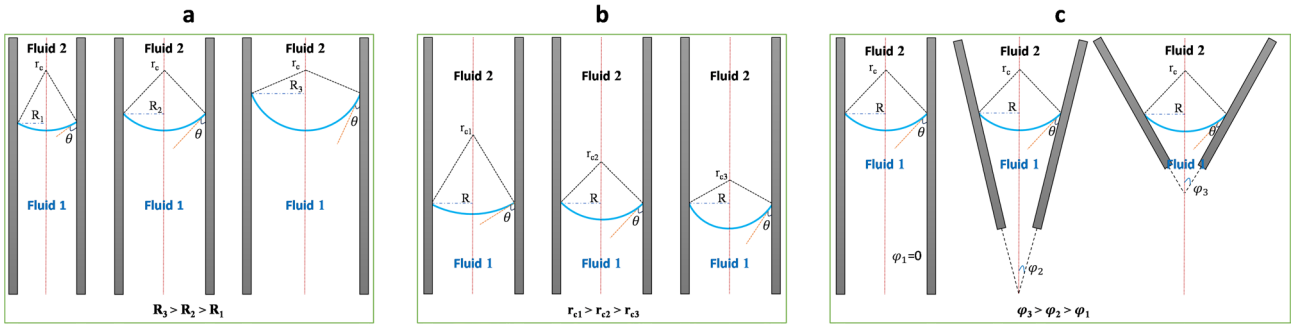

Fig. 11. The effect of (**a**) pore radius (R), (**b**) fluid interface curvature (r_c), and (**c**) convergence angle of the pores (φ) on the contact angle of a rough surface.

Mean roughness (μm)	Contact angle hysteresis (degree)		
	DW-Air	Brine-Air	CO-Air
30.37	13.14	6.39	0
28.90	12.49	12.88	0
16.48	0	0	7.83
6.75	0	0	10.13
5.31	0	0	9.44

Table 9. Effect of surface roughness on contact angle hysteresis in the liquid-air-solid system for DW, Brine, and CO under ambient conditions.

shown in Fig. 10, depending on the trapped fluid—whether it is a wetting or non-wetting fluid the receding contact angle can be associated with either negative or positive pressure, which is the capillary pressure.

$$\theta = cos^{-1}\left(\frac{R}{r_c}\right) - \varphi \tag{7}$$

θ: Contact angle, φ: Convergence angle of the pores, r_c: Curvature of the interface, R: Pore radius at the wetting front.

Evaluation of contact angle hysteresis

Surface roughness plays a critical role in influencing the dynamics of the contact line, which is the boundary where a liquid interface meets a solid surface. This interaction is central to processes such as wetting, spreading, and droplet motion[41–43]. Contact angle hysteresis (CAH) is a parameter that indicates how a drop moves across a surface. The CAH presented in Table 9 demonstrates a uniform process of increasing surface roughness for different fluids. When the difference between the advancing contact angle and the receding contact angle (i.e., the CAH) is low, the drop moves more easily along the contact line. Conversely, when the CAH increases due to the drop pinning at certain locations, more force is required to move the contact line. Roughness can cause the contact line to pin, where it becomes stuck at certain points due to energy barriers created by surface irregularities, leading to discontinuous or jerky motion[41–43]. The motion of the three-phase contact line can be influenced by various factors, including surface roughness, surface roughness profile, fluid properties (such as surface tension and viscosity), and the fluid trapped beneath the drop. Increasing surface roughness can enhance the potential for pinning the contact line; however, the roughness profile can also affect the motion of the contact line, depending on the position of the drop.

The increase in viscosity of the fluid in droplet form, as well as an increase in surface tension, will resist the movement of the contact line and affect the motion of the three-phase contact line. However, overcoming structural forces, along with the capillary forces created by rough surfaces, has a more dominant effect on resistance to surface tension and fluid viscosity. Moreover, surface roughness can either enhance or reduce wetting, depending on its structure. Hierarchical roughness, which combines micro- and nano-scale features, can lead to superhydrophobic or superhydrophilic behavior, significantly altering contact line dynamics. Roughness also increases the effective surface area, which can enhance wetting if the liquid fully wets the surface, or reduce it if air pockets are trapped beneath the liquid, as in the Cassie-Baxter state. During dynamic wetting or dewetting, roughness can cause stick-slip motion, where the contact line intermittently sticks to surface features before jumping forward or backward. Finally, roughness modifies the apparent contact angle, influencing the driving forces for contact line motion and thereby affecting its overall dynamics in either the Wenzel or Cassie-Baxter wetting regimes[41–43].

The evaluation of the CAH values presented in Table 9 shows that the dynamics of the contact line can result in different values depending on the surface morphology. The complex morphology and geometry of the rough surface, as shown in Table 3, cause some areas to be completely filled with liquid droplets while others trap air. This situation is representative of the Wenzel and Cassie-Baxter models, which coexist in the studied systems (Fig. 9). The changes in the CAH values in Table 9 reflect this phenomenon, as they vary with increasing roughness. The CAH results indicate that when the values are low, the movement of the contact line is easier. This ease of movement may be due to the trapping of air, which facilitates the contact line's motion and is indicative of the Cassie-Baxter model. Conversely, an increase in CAH may result from the filling of surface roughness with droplet fluid, leading to pinning of the contact line, which is characteristic of the Wenzel model. In this case, higher CAH values are observed due to the adhesion of the contact line. The trend in changes in contact angle hysteresis with respect to increasing surface roughness has not been uniform, which can be attributed to the complex morphology of the surface. This complexity has led to the simultaneous behavior of the Wenzel and Cassie-Baxter models occurring in different parts of the droplet contact line[35,36].

Evaluation of the effect of fluid type

In addition to structural forces, the contact angle is affected by van der Waals and electrostatic forces, which help maintain a film of fluid on the surface in equilibrium[44,45]. Van der Waals forces between the surface and the fluid are dominant when the fluid interacts with a non-charged surface and significantly influence the contact angle. The presence of polar components in the fluid, as well as the charge of the surface, induces electrostatic

repulsion and attraction, which affects the stability of the fluid on the surface and the contact angle[44,45]. The surface used in this study is made of silicon carbide, which has an isoelectric point (pH) of 4 to 6[46–48]. In the systems evaluated, the surface charge of silicon carbide has consistently been negative. In the liquid-air-solid system, the surfaces exposed to the bulk air have a negatively charged surface due to oxidation. Additionally, in the liquid-liquid-solid system, since the bulk of deionized water or brine has a pH higher than the isoelectric point of silicon carbide, this results in a negatively charged silicon carbide surface. The charge of the surface leads to electrostatic attraction and repulsion between the surface and the fluid, which, along with van der Waals forces, influences the contact angle. The fluids evaluated, each with different chemical properties and charged components, create varying molecular interactions with the surface through van der Waals and electrostatic forces. These interactions, along with structural forces and surface and interfacial tension, result in changes to the contact angle. Reducing surface tension and creating electrostatic attraction lead to a lower contact angle (indicating greater affinity of the surface for the fluid). Conversely, electrostatic repulsion can also cause an increase in the contact angle. Changes in roughness and the surface roughness profile in both liquid-air-solid and liquid-liquid-solid systems alter the interactions between the surface and the fluid, including electrostatic and van der Waals interactions. These changes arise from variations in the contact area of the droplet with the rough surface, subsequently affecting the behavior of the contact angle.

Van der Waals forces include three types of interactions: Keesom, Debye, and London. These interactions occur between the surface and the fluid, as well as between the fluids themselves, and can affect the contact angle[44,45]. In a liquid-air-surface system, the interaction between trapped air and polar fluids (DW, brine, CO) is primarily a Debye interaction, while the London interaction occurs between air and a nonpolar fluid (n-heptane). CO, despite having nonpolar components, also contains polar components such as asphaltenes and resins, which lead to both Debye and London interactions occurring simultaneously. The results obtained for different fluids (Table 5) evaluated in the liquid-air-solid system indicate that increasing the polarity of the fluid is associated with an increase in the contact angle. The nature of DW and brine as water-based fluids, as well as CO and n-heptane as oil-based fluids, is comparable. Dissolving salt in water increases the polar components in water, resulting in a higher polarity for brine compared to DW. Additionally, the presence of asphaltene and resin, which are polar components in oil, in CO compared to n-heptane (a nonpolar fluid) results in CO having a higher polarity than n-heptane. Increasing the polarity of the fluid in the liquid-air-solid system shows that by intensifying the Debye interaction and weakening the London interaction, the contact angle increases and wettability decreases. The complete dispersion of n-heptane on the evaluated surfaces indicates the dominance of London interactions, leading to a stronger affinity between the surface and the nonpolar fluid. However, in the liquid-liquid-solid system (Table 6), the bulk fluid is a polar component, which causes the interaction between CO as a droplet fluid and DW or brine as trapped fluids to be dominated by Debye interactions. The Debye interaction occurs between an induced dipole and a permanent dipole, and it is intensified by increasing polarity. The strengthening of the Debye interaction in the liquid-liquid-solid system causes a decrease in the contact angle and an increase in wettability for the CO-brine-solid system compared to the CO-DW-solid system. These interactions also highlight the importance of the trapped fluid and indicate that the trapped fluid significantly impacts the contact angle on a rough surface.

The differences in contact angle values observed in the liquid-liquid-solid system for brine and DW are related to the characteristics of the rough surface, as well as the nature of the surface chemistry and the liquids involved. The change in fluid charge for DW and brine results in different interactions between the ions in brine and the charged surface. The significance of the difference in contact angle values for DW and brine lies in the interaction between the hydration shell of ions in brine. Recent studies by various researchers have highlighted the interactions between the polar components of oil, the hydration shell of ions in fluid-fluid interactions, and the charged surface with the hydration shell of ions during surface-fluid interactions[49–53]. The interactions between OH^- in the anion hydration shell and H^+ in the cation hydration shell with the polar components of a fluid, as well as with a charged surface, can affect interfacial tension and contact angle. The interaction between the hydration shell and the surface, along with other charged fluids including oil, is related to the hydration energy of the ions present in water and their quantity. The brine investigated in this study contains Na^+ and Cl^- ions, whose hydration energy and the number of water molecules in their hydration shells can influence the interaction of brine with the surface, in addition to the quantity of each ion. The hydration energy of Na^+ (the absolute value of the hydration energy) and the number of water molecules in its hydration shell are greater than those of Cl^-[49,54]. Given that the surface evaluated in this study has a negatively charged surface, its interaction with the hydration shell of the Na^+ cation in brine is likely to be stronger. The negatively charged surface tends to attract the hydration shell of the cation and its H^+ ions. Furthermore, due to the higher hydration energy of Na^+ compared to Cl^-, the potential for surface interaction with Na^+ will be greater than that with Cl^-. Additionally, the interaction between the polar components of oil and brine, due to the greater polarity of brine and the tendency of the polar components of oil to interact with the hydration shell of brine ions, results in CO being more attracted to the rough surface where brine is trapped than to DW. Consequently, the contact angle for the CO-brine-solid system will be lower than that for the CO-DW-solid system.

Physical description of the empirical model

The presented model (Equation) demonstrates the nonlinear and complex behavior of the contact angle concerning mean roughness, which can yield different outcomes depending on the type of fluid and the system under consideration. According to the Equation, when the mean roughness is zero, the contact angle reflects a smooth surface (zero roughness), represented by the coefficient *a*. The interaction between the surface and the fluids, as well as between the fluids themselves on a smooth surface, is captured in the constant coefficient *a*. The tension between the surface and the droplet, along with the bulk fluid, as well as the evaluated surface tension or interfacial tension, indicates the effect of the chemistry of the surface and the fluid and their interactions. In the

liquid-air-solid system, the tendency of the surface to attract the fluid at zero roughness has caused the droplet to spread completely on the surface, which is also reflected in the values of *a*. However, in the liquid-liquid-solid system, the change of the bulk fluid from air to DW or brine has significantly altered and reduced the tension between the surface and the bulk fluid. Additionally, the interfacial tension between the two liquids is lower than the surface tension (air-liquid). The decrease in interfacial tension leads to a reduction in the contact angle, whereas the decrease in tension between the surface and the bulk results in an increase in the contact angle (according to Eq. 1). This interaction has ultimately caused the contact angle on the smooth surface in the liquid-liquid-solid system to be greater than that in the liquid-air-solid system, indicating that the decrease in tension between the surface and the bulk prevails.

Conclusions

This study reveals that wettability arises from the synergistic interplay of surface roughness, fluid chemistry, and multiphase interactions, rather than isolated surface properties. While roughness consistently alters contact angles across systems, its effects are fluid-specific: aqueous systems (DW/brine-air) exhibit amplified hydrophobicity with roughness, particularly under brine's electrolyte-mediated ionic effects, while hydrocarbons display divergent behaviors enhanced crude oil adhesion versus negligible roughness sensitivity for n-heptane. In oil-water systems, roughness paradoxically elevates water affinity while favoring oil-wet states, with brine further modulating wettability through ion-specific interfacial competition. These results challenge classical wettability models (e.g., Wenzel, Cassie-Baxter), which fail to account for dynamic fluid-topography-chemistry coupling, necessitating advanced frameworks that integrate heterogeneous surface energetics, fluid polarity, and ionic dynamics. Understanding how surface roughness impacts crude oil contact angles on reservoir rocks is vital for optimizing oil recovery and flow management. Roughness modifies wettability to enhance oil displacement, reduces capillary trapping, and improves reservoir modeling accuracy. It also enables tailored engineering solutions for shale production and pipeline fouling prevention, directly boosting operational efficiency in petroleum systems. Future efforts must unravel molecular-scale interactions at rough interfaces to enable predictive control of wettability in complex environments.

Data availability

All data generated or analyzed during this study is included in this published article.

Received: 16 January 2025; Accepted: 5 May 2025
Published online: 13 May 2025

References

1. Good, R. J. Contact angle, wetting, and adhesion: A critical review. *J. Adhes. Sci. Technol.* **6**, 1269–1302 (1992).
2. Prabhu, K. N., Fernades, P. & Kumar, G. Effect of substrate surface roughness on wetting behaviour of vegetable oils. *Mater. Des.* **30**, 297–305 (2009).
3. Borruto, A., Crivellone, G. & Marani, F. Influence of surface wettability on friction and wear tests. *Wear* **222**, 57–65 (1998).
4. Genzer, J. & Efimenko, K. Recent developments in superhydrophobic surfaces and their relevance to marine fouling: A review. *Biofouling* **22**, 339–360 (2006).
5. Roucoules, V., Gaillard, F., Mathia, T. & Lanteri, P. Hydrophobic mechanochemical treatment of metallic surfaces: Wettability measurements as a means of assessing homogeneity. *Adv. Colloid Interface Sci.* **97**, 179–203 (2002).
6. Wenzel, R. N. Resistance of solid surfaces to wetting by water. *Ind. Eng. Chem.* **28**, 988–994 (1936).
7. Chow, T. Wetting of rough surfaces. *J. Phys. Condens. Matter* **10**, L445 (1998).
8. Kaplan, W. D., Chatain, D., Wynblatt, P. & Carter, W. C. A review of wetting versus adsorption, complexions, and related phenomena: The Rosetta stone of wetting. *J. Mater. Sci.* **48**, 5681–5717 (2013).
9. Vijapurapu, C. S., Rao, D. N. & Kun, L. in *SPE Improved Oil Recovery Conference?* (SPE-75211-MSSPE, 2002).
10. Whyman, G., Bormashenko, E. & Stein, T. The rigorous derivation of young, Cassie–Baxter and Wenzel equations and the analysis of the contact angle hysteresis phenomenon. *Chem. Phys. Lett.* **450**, 355–359 (2008).
11. Arsalan, N., Buiting, J. J. & Nguyen, Q. P. Surface energy and wetting behavior of reservoir rocks. *Colloids Surf. Physicochem. Eng. Aspects* **467**, 107–112 (2015).
12. Babadagli, T., Raza, S., Ren, X. & Develi, K. Effect of surface roughness and lithology on the water–gas and water–oil relative permeability ratios of oil-wet single fractures. *Int. J. Multiph. Flow* **75**, 68–81 (2015).
13. Li, Z. et al. Wetting and spreading behaviors of nanodroplets: The interplay among substrate hydrophobicity, roughness, and surfactants. *J. Phys. Chem. C.* **120**, 15209–15215 (2016).
14. Scanziani, A., Singh, K., Blunt, M. J. & Guadagnini, A. Automatic method for estimation of in situ effective contact angle from X-ray micro tomography images of two-phase flow in porous media. *J. Colloid Interface Sci.* **496**, 51–59 (2017).
15. Nowrouzi, I., Manshad, A. K. & Mohammadi, A. H. Effects of dissolved binary ionic compounds and different densities of Brine on interfacial tension (IFT), wettability alteration, and contact angle in smart water and carbonated smart water injection processes in carbonate oil reservoirs. *J. Mol. Liq.* **254**, 83–92 (2018).
16. Siddiqui, M. A. Q., Ali, S., Fei, H. & Roshan, H. Current understanding of shale wettability: A review on contact angle measurements. *Earth-Sci. Rev.* **181**, 1–11 (2018).
17. Sun, R., Xiao, H. & Sun, H. Investigating the settling dynamics of cohesive silt particles with particle-resolving simulations. *Adv. Water Resour.* **111**, 406–422 (2018).
18. Huang, N., Liu, R., Jiang, Y., Li, B. & Yu, L. Effects of fracture surface roughness and shear displacement on geometrical and hydraulic properties of three-dimensional crossed rock fracture models. *Adv. Water Resour.* **113**, 30–41 (2018).
19. Wang, X. & Zhang, Q. Insight into the influence of surface roughness on the wettability of apatite and dolomite. *Minerals* **10**, 114 (2020).
20. Sari, A., Al Maskari, N. S., Saeedi, A. & Xie, Q. Impact of surface roughness on wettability of oil-brine-calcite system at sub-pore scale. *J. Mol. Liq.* **299**, 112107 (2020).
21. Jiang, H., Guo, B. & Brusseau, M. L. Characterization of the micro-scale surface roughness effect on immiscible fluids and interfacial areas in porous media using the measurements of interfacial partitioning tracer tests. *Adv. Water Resour.* **146**, 103789 (2020).
22. Alnoush, W., Sayed, A., Solling, T. I. & Alyafei, N. Impact of calcite surface roughness in wettability assessment: Interferometry and atomic force microscopy analysis. *J. Pet. Sci. Eng.* **203**, 108679 (2021).

23. Nikoo, A. H. & Malayeri, M. R. On the affinity of carbonate and sandstone reservoir rocks to scale formation—Impact of rock roughness. *Colloids Surf. Physicochem. Eng. Aspects* **610**, 125699 (2021).
24. Alqam, M. H., Abu-Khamsin, S. A., Sultan, A. S., Al-Afnan, S. F. & Alawani, N. A. An investigation of factors influencing carbonate rock wettability. *Energy Rep.* **7**, 1125–1132 (2021).
25. Sun, Y. et al. Effect of surface roughness on particle-bubble interaction: A critical review. *Minerals Eng.* **201**, 108223 (2023).
26. Hay, K., Dragila, M. & Liburdy, J. Theoretical model for the wetting of a rough surface. *J. Colloid Interface Sci.* **325**, 472–477 (2008).
27. Kubiak, K., Mathia, T. & Wilson, M. in *Proceedings of the Fourteenth International Congress of Metrology, Paris, France*, Vol. 22 (2009).
28. Azizian, S. & Khosravi, M. in *Interface Science and Technology*, Vol. 30 283–332 (Elsevier, 2019).
29. Tran, P. A. & Webster, T. J. Understanding the wetting properties of nanostructured selenium coatings: The role of nanostructured surface roughness and air-pocket formation. *Int. J. Nanomed.* 2001–2009 (2013).
30. McHale, G. Cassie and Wenzel: Were they really so wrong? *Langmuir* **23**, 8200–8205 (2007).
31. Liu, J., Mei, Y. & Xia, R. A new wetting mechanism based upon triple contact line pinning. *Langmuir* **27**, 196–200 (2011).
32. Marmur, A. & Bittoun, E. When Wenzel and Cassie are right: Reconciling local and global considerations. *Langmuir* **25**, 1277–1281 (2009).
33. Gao, L. & McCarthy, T. J. How Wenzel and Cassie were wrong. *Langmuir* **23**, 3762–3765 (2007).
34. Li, H., Feng, X. & Zhang, K. Study of the classical Cassie theory and Wenzel theory used in nanoscale. *J. Bion. Eng.* **18**, 398–408 (2021).
35. Jiang, Y. & Xiao, Y. A unified model for droplet receding contact angles on hydrophobic pillar, pore, and hollowed pillar arrays. *J. Colloid Interface Sci.* **683**, 869–876 (2025).
36. Jiang, Y., Xiao, Y. & Wei, C. Sticky superhydrophobic state. *J. Phys. Chem. Lett.* **15**, 11896–11902 (2024).
37. Behnoudfar, D., Dragila, M. I., Meisenheimer, D. & Wildenschild, D. Contact angle hysteresis: A new paradigm? *Adv. Water Resour.* **161**, 104138 (2022).
38. Dullien, F. A. *Porous Media: Fluid Transport and Pore Structure* (Academic Press, 2012).
39. Jin, M. et al. Superhydrophobic aligned polystyrene nanotube films with high adhesive force. *Adv. Mater.* **17**, 1977–1981 (2005).
40. Jiang, Y., Xu, Z., Li, B., Li, J. & Guan, D. Soft wetting: Droplet receding contact angles on soft superhydrophobic surfaces. *Langmuir* **39**, 15401–15408 (2023).
41. Randive, P., Dalal, A., Sahu, K. C., Biswas, G. & Mukherjee, P. P. Wettability effects on contact line dynamics of droplet motion in an inclined channel. *Phys. Rev. E.* **91**, 053006 (2015).
42. Sadeghinezhad, E., Siddiqui, M. A. Q., Roshan, H. & Regenauer-Lieb, K. On the interpretation of contact angle for geomaterial wettability: Contact area versus three-phase contact line. *J. Pet. Sci. Eng.* **195**, 107579 (2020).
43. Zheng, W., Wen, B., Sun, C. & Bai, B. Effects of surface wettability on contact line motion in liquid–liquid displacement. *Phys. Fluids* **33** (2021).
44. Butt, H. J. & Kappl, M. *Surface and Interfacial Forces* (Wiley, 2018).
45. Israelachvili, J. N. *Intermolecular and Surface Forces* (Academic Press, 2011).
46. Cai, K. et al. Geometrically complex silicon carbide structures fabricated by robocasting. *J. Am. Ceram. Soc.* **95**, 2660–2666 (2012).
47. Rao, R. R., Roopa, H. & Kannan, T. Effect of pH on the dispersability of silicon carbide powders in aqueous media. *Ceram. Int.* **25**, 223–230 (1999).
48. Wu, Y. F. & Chen, Y. M. Separation of silicon and silicon carbide using an electrical field. *Sep. Purif. Technol.* **68**, 70–74 (2009).
49. Abdi, A., Awarke, M., Malayeri, M. R. & Riazi, M. Interfacial tension of smart water and various crude oils. *Fuel* **356**, 129563 (2024).
50. Abdi, A., Ranjbar, B., Kazemzadeh, Y., Aram, F. & Riazi, M. Investigating the mechanism of interfacial tension reduction through the combination of low-salinity water and bacteria. *Sci. Rep.* **14**, 11408 (2024).
51. Ahmadi Aghdam, M., Riahi, S. & Khani, O. Experimental study of the effect of oil Polarity on smart waterflooding in carbonate reservoirs. *Sci. Rep.* **14**, 22190 (2024).
52. Ahmadi, B., Molaei, A. H., Sahraei, E. & Mohammadi, A. H. Evaluation of competitive and synergistic effects of potential determining ions on interfacial tension reduction and wettability alteration in carbonate oil reservoirs. *Colloids Surf. Physicochem. Eng. Aspects* **713**, 136474 (2025).
53. Ahmadi, B., Molaei, A. H., Sahraei, E. & Mohammadi, A. H. Exploring the effects of salinity and ionic composition on wettability alteration and interfacial properties in carbonate oil reservoirs. *Colloids Surf. Physicochem Eng. Aspects*, 136554 (2025).
54. Marcus, Y. Thermodynamics of solvation of ions. Part 5—Gibbs free energy of hydration at 298.15 K. *J. Chem. Soc. Faraday Trans.* **87**, 2995–2999 (1991).

Author contributions

M. Razavifar: Methodology, Data curation, Investigation, Formal analysis, Writing original draft. A. Abdi: Methodology, Data curation, Investigation, Validation, review and editing. E. Nikooee: Supervision, review and editing. O. Aghilie: Investigation, Writing original draft.M. Riazi: Supervision, Conceptualization, Validation, review and editing.

Declarations

Competing interests

The authors declare no competing interests.

Additional information

Correspondence and requests for materials should be addressed to M.R.

Reprints and permissions information is available at www.nature.com/reprints.

Publisher's note Springer Nature remains neutral with regard to jurisdictional claims in published maps and institutional affiliations.